HHS Public Access

Author manuscript

Lab Chip. Author manuscript; available in PMC 2020 June 07.

Published in final edited form as:

Lab Chip. 2019 June 07; 19(11): 1977–1984. doi:10.1039/c9lc00054b.

On-the-fly Exchangeable Microfluidic Nozzles for Facile Production of Various Monodisperse Micromaterials

Tom Kamperman[†,*], **Bas van Loo**[†], **Melvin Gurian**, **Sieger Henke**, **Marcel Karperien**, and **Jeroen Leijten**[*]

Department of Developmental BioEngineering, Faculty of Science and Technology, Technical Medical Centre, University of Twente, Drienerlolaan 5, 7522 NB Enschede, The Netherlands.

Abstract

Microfluidic manufacturing platforms have advanced the production of monodisperse, shape-controlled, and chemically defined micromaterials. However, conventional microfabrication platforms are typically designed and fabricated as single-purpose and single-use tools, which limits their efficiency, versatility, and overall potential. We here present an on-the-fly exchangeable nozzle concept that operates in a transparent, 3D, and reusable microfluidic device produced without cleanroom technology. The facile exchange and repositioning of the nozzles readily enables the production of monodisperse water-in-oil and oil-in-water emulsions, solid and core-shell microspheres, microfibers, and even Janus type micromaterials with controlled diameters ranging from 10 to 1000 μm using a single microfluidic device.

TOC Graphic

Exchangeable microfluidic nozzles enable the facile production of a wide variety of micromaterials using a single cleanroom-free manufactured microfluidic device.

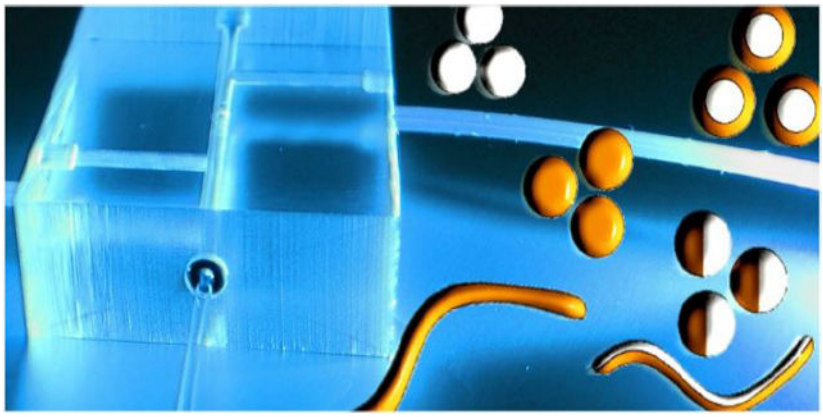

[*] t.kamperman@utwente.nl; jeroen.leijten@utwente.nl.

[†] Co-first authors / contributed equally to this work

Conflicts of interest

There are no conflicts of interest to declare.

Electronic Supplementary Information (ESI) available: Experimental section, Figure S1–5, Movie S1. See DOI: 10.1039/x0xx00000x

Introduction

Microfluidic devices offer predictable (i.e., laminar) flow behaviour, in-line manipulation, and monitoring of liquids.[1] This control over liquids has enabled the production of micromaterials with controlled size, shape, and composition.[2–4] Microfluidic devices are typically produced as channels that are permanently formed and/or enclosed within glass or transparent polymer using a covalent bonding strategy such as plasma bonding, gluing, or fusing via partial melting or dissolving.[5, 6] The non-reversible nature of these conventional microfluidic device fabrication methods limits their use to a single specific application. In particular, device dimensions and surface wetting properties need to be optimized per application, with little to no flexibility for efficient adaptation to other applications.[7, 8] Conventional microfluidic devices are also inefficient during design optimization strategies, as their non-adaptable nature hampers swift iterations towards a functional device. On top, conventional microdevices are considered as single-use disposables. Cleaning difficulties of permanently bonded devices contributes to significant wastage of (e.g., clogged) chips, which is highly cost-inefficient considering the high-end materials, skilled personnel, and advanced lithographic infrastructure that are typically required for manufacturing of microfluidic devices. These limitations have jointly been hampering the rapid and widespread adoption of microfluidic technologies into other scientific disciplines as well as translation into clinical and industrial applications.[9, 10]

Opportunely, microfluidic devices with on-demand adaptable channels represent a straightforward flexible solution to expand the versatility and efficiency of microfluidic devices. Reusable ‘off-the-shelf’ microfluidic devices made from plastic parts and steel needles have been explored to this end. These devices have been successfully used for flow focusing applications,[11] generation and splitting of water-in-oil (W/O) droplets,[12, 13] and liposome generation.[14] However, the non-transparent nature of current devices impaired the direct monitoring that is required for controlled droplet formation and manipulation processes. Nozzle positioning has, for example, a major effect on the droplet size.[15] Furthermore, microfluidic device transparency is critical for the on-chip photocrosslinking of various polymers.[16] The pressing need for on-the-fly adoptable microfluidic devices is furthermore reflected by the recent development of several modular microfluidic systems.[17–20] Regardless of their promise, current adaptable microfluidic devices are not yet readily compatible with the production of solid micromaterials.

In this work, we demonstrate the fabrication of monodisperse micrometer-sized droplets, beads, and fibers using a fully transparent multifunctional 3D microfluidic device with exchangeable nozzles. The microfluidic device was manufactured without cleanroom technology and could be configured on-the-fly to operate in a T-junction, coaxial flow, and flow focusing manner. Combining this multifunctional microfluidic production platform with various classes of *in situ* crosslinkable polymers enabled the straightforward micromanufacturing of myriad micromaterials with controlled size, shape, composition, and complexity (Figure 1).

Results and Discussion

Design and fabrication of multifunctional microfluidic device with exchangeable nozzles

The microfluidic device design consisted of a center channel and two side channels that essentially formed two serially connected T-junctions (Figure 2a). This design was compatible with the user-defined assembly of a variety of nozzles into the three most used nozzle configurations, namely T-junction, coaxial flow, and flow focusing, and thus acted as a universal platform for the fabrication of a variety of micromaterials.

The device was fabricated in polymethylmethacrylate (PMMA), as this material is transparent, widely available, and biocompatible, but also mechanically robust while easily adaptable using standard cutting and abrasion methods. Channels were micromilled in the presence of concentrated soap solution that acted as a coolant and prevented heat-induced cracking of the PMMA, resulting in precise and highly reproducible microfluidic device fabrication (Figure 2b).[21] Channels were measured to be 0.9 mm in diameter, which allowed for the insertion of a wide variety of commercially available capillaries. The device inlets and outlets consisted of 1.6 mm wide holes that enabled the insertion of 1/16” (i.e., ~1.59 mm) outer diameter tubing, which is commonly used in microfluidic applications. After micromilling, the transparency of the center channel was increased by >2.5-fold through abrasion using a knotted thread and polish (Figure 2c and Figure S1).

Fused silica capillaries were selected as nozzles, as they are readily available with inner diameters ranging from 2±1 to 700±10 μm and outer diameters ranging from 90±6 to 850±20 μm, thus nearly spanning the entire micrometer regime. Furthermore, fused silica capillaries can be pre-coated with, for example, a polyimide layer to improve durability and provide UV-protection. Exchangeable nozzles were fabricated by gluing a fused silica capillary into 1/16” tubing (i.e., for T-junction and coaxial flow) or by inserting it into silicone tubing (i.e., for flow focusing), which acted as outlet tubing (Figure S2). The transparent and semi-permeable nature of the silicone outlet tubing enabled in-line monitoring, photo-irradiation of the flowing materials, and diffusion-based delivery of small molecules such as reactive hydrogen peroxide to induce or control chemical reactions.[22]

The microfluidic device inlets and outlets were partially widened to hold elastic O-rings that formed liquid tight seals and ensured centring of the exchangeable nozzles and/or tubing in the microfluidic device’s channels. Optionally, a borosilicate glass capillary spacer was used to enable sealing of the silicone tubing into the device. As expected, the PMMA device and rubber O-rings enabled the facile connection of tubing and fused silica nozzles in various configurations, as confirmed by successful demonstration of W/O emulsification using T-junction, coaxial, and flow focusing modes, as well as the formation of a focused aqueous two-phase coaxial flow (Figure 2d–h).

Expanding the microfluidic droplet production regime using exchangeable nozzles

Microfluidic droplets can be leveraged as templates for the controlled fabrication of microspheres.[23] The size of such microfluidic-generated materials strongly depends on the nozzle width, the flow ratio of the dispersed and continuous phases, and (for droplet and particles) the capillary number of the continuous phase $Ca = \eta_c v_c / \gamma$, where η_c is the

viscosity of the continuous phase, v_c is the average velocity of the continuous phase, and γ is the interfacial tension between the dispersed and continuous phases.[24] Tuning the flow rates of the dispersed and continuous phases is thus a potent strategy to control the droplet size. However, stable production of monodisperse droplets is limited to the squeezing and dripping regimes.[25, 26] Therefore, droplet size can only be fine-tuned within a relatively small regime, typically limited to an order of magnitude in diameter.[27–29] We hypothesized that the production regime of a single microfluidic device could be significantly expanded in terms of droplet size by controlling the nozzle diameter on-the-fly. To demonstrate this, our microfluidic device was successively equipped with three different nozzles (D_{nozzle} = 75, 200, 700 μm) during a continuous experiment. On-the-fly exchange of the nozzles readily enabled the production of monodisperse microdroplets with diameters exceeding an order of magnitude, as demonstrated by emulsification of water in a 1% Span 80 containing hexadecane solution (Figure 3a). The rubber O-rings enabled facile and swift nozzle exchange by guaranteeing instant sealing and auto-centring of the nozzles, which allowed for the switching between different droplet size production regimes in less than a minute (Figure 3b, Movie S1). As expected, with every nozzle the droplet size could be fine-tuned by controlling the capillary number. Specifically, increasing the capillary number by increasing the continuous phase flow rate resulted in reduction of the droplet size (Figure 3c–e). Furthermore, the exact position of nozzles significantly affected the droplet production regime, which could be uniquely simultaneously fine-tuned and monitored through on-the-fly repositioning of the nozzles within our transparent microfluidic device (Figure S3). Microdroplets over the entire size regime were characterized by a monodisperse size distribution as confirmed by coefficients of variation CV <5%. (Figure 3f). Similar size control was achieved with all-aqueous two-phase co-flows, which is key for the microfabrication of, for example, microfibers with controlled diameters (Figure S4).

Chemical and physical nozzle tuning for micromaterial production

Controlling microfluidic nozzle wettability is key to achieve successful generation of droplets. The fused silica nozzles used in this work contain siloxane bridges that bind water via chemisorption to form silanol groups, which adsorb polar compounds including water molecules allowing it to act as a hydrophilic surface.[30] Consequently, fused silica is inherently hydrophilic in its native state, which was confirmed by contact angle measurements (θ = 27±5°) using the capillary rise method (Figure 4a).[31] Fused silica nozzles were therefore readily compatible with production of oil-in-water (O/W) emulsions such as hexadecane in a 1% sodium dodecyl sulphate (SDS) containing water solution. However, the nozzles' hydrophilic nature also hampered the stable formation of W/O emulsions. Moreover, aqueous wetting of fused silica was exacerbated in the presence of water-soluble polymers such as dextran, which hindered the formation of microsphere precursor droplets (Figure 4a). To enable polymer microsphere formation through microfluidic emulsion templating using our microfluidic platform, fused silica nozzles were deactivated by chemically coupling fluorinated silane to the available silanol groups (Figure 4b) The fluorinated fused silica nozzles were significantly less hydrophilic (θ = 52±2°) than pristine fused silica nozzles and were proven to be compatible with the W/O emulsification of 5% dextran solution (Figure 4c).

Besides chemical modification, exchangeable nozzles could also be physically optimized for the processing of polymer precursor solutions. For example, selectively modifying the optical properties of nozzles offers the possibility to optimize the microfluidic system for processing photocrosslinkable polymers. An ongoing challenge in on-chip photocrosslinking strategies is microfluidic channel clogging due to photocrosslinking of polymers by strayed UV light.[32–34] To overcome UV-induced clogging, we exchanged the conventionally used glass or borosilicate capillaries by polyimide-coated fused silica capillaries that acted as UV-protected nozzles (Figure 4d,e). Absorption spectrometry confirmed that polyimide-coated nozzles absorbed significantly more UV light (λ = 365 nm) than pristine fused silica nozzles (Figure 4f). Advantageously, the polyimide-coated nozzles enabled the continuous and stable on-chip production of polyethylene glycol diacrylate (PEGDA) microdroplets in the presence of UV light, while the pristine nozzle mainly associated with clogging (Figure 4g,h). Moreover, the use of polyimide-coated nozzles significantly widened the operational window for the production of completely photocrosslinked PEGDA microspheres (Figure 5i).

On-demand fabrication of a wide variety of micromaterials

To demonstrate the universal nature of the microfluidic device, it was combined with a variety of nozzles in different configurations to produce various different classes of micromaterials. To this end, several combinations of distinct (i) polymers (natural and synthetic); (ii) crosslinking mechanisms (chemical and physical); (iii) morphologies (spherical and fiber); and (iv) complexities (isotropic solid, Janus solid, and core-shell) were produced (Figure 5).

A flow focusing configuration of a fluorinated fused silica nozzle enabled the stable production of isotropic solid and core-shell dextran microspheres (Figure 5a). Specifically, a mixture of dextran-tyramine (Dex-TA) and horseradish peroxidase (HRP) was emulsified with hexadecane that contained Span 80, and flown through a semi-permeable silicone tubing that was submerged in H_2O_2. Diffusion-based supplementation of H_2O_2 into the polymer droplets initiated the enzymatic crosslinking of the tyramine moieties resulting in the formation of monodisperse dextran microspheres.[22] Core-shell microspheres were produced by adding the H_2O_2 consuming enzyme catalase to the polymer solution,[35, 36] which prevented crosslinking of the droplet center.

A polyimide-coated capillary in coaxial flow mode was used as a UV-shielded nozzle to demonstrate the stable production of photocrosslinked PEGDA microspheres (Figure 5b). Acrylate moieties of PEGDA can be covalently coupled through free-radical polymerization upon irradiation of a photoinitiator such as 2-Hydroxy-4′-(2-hydroxyethoxy)-2-methylpropiophenone (I2959). Straightforward W/O emulsification of a PEGDA and I2959 containing solution using a UV-irradiated coaxial flow nozzle resulted in the stable and clog-free formation of monodisperse PEGDA microspheres. A combination of coaxial flow and flow focusing was used to generate alginate microspheres (Figure 5c). Specifically, this nozzle arrangement enabled the formation of a laminar three-layered co-flow of $CaCO_3$ nanoparticles in alginate, Span 80 in hexadecane, and Span 80 and acetic acid in hexadecane. The alginate droplets were ionically crosslinked using divalent calcium cations,

which were released upon the acid-induced dissolution of $CaCO_3$.[37] The middle oil flow acted as a liquid barrier between the $CaCO_3$ and the acetic acid, which prevented clogging of the microfluidic device. Alginate microfibers were produced using the same nozzle configuration by coflowing solutions of alginate, polyethylene glycol (PEG) and $CaCl_2$. The middle PEG flow acted as a liquid barrier between the divalent calcium ions and the alginate, which prevented microfluidic device clogging. Inserting a multibore nozzle readily provided an extra level of complexity, as demonstrated by the production of Janus type microfibers (Figure 5c and Figure S5).

Conclusions

Microfluidic platforms for micromaterial production typically rely on permanently enclosed single-use devices with limited operational freedom. In this work, we presented a re-usable microfluidic device with disposable exchangeable nozzles, which enabled the controlled production of a wide variety of micromaterials. The device was fabricated in PMMA using standard cutting and abrasion methods that do not demand clean-room infrastructures. Reversible exchange of the tubing, nozzles, and device was enabled in a rapid, straightforward, and leak-free manner. On-the-fly nozzle exchange enabled the continuous generation of microfluidic products over a size range far exceeding the production limits of conventional fixed nozzle devices. Furthermore, nozzle exchange readily allowed for the tuning of surface wetting properties, which enabled swift iteration towards functional micromanufacturing protocols for various materials. Various nozzle configurations, materials, and crosslinking methods have been efficiently and successfully combined to demonstrate the user-friendly manufacturing of a myriad of micromaterials. Uniquely, equipping the transparent microfluidic device with UV-protected nozzles enabled the stable production of photocrosslinked polymer microspheres. The universal and facile nature of the transparent 3D microfluidic device with exchangeable nozzles is expected to facilitate the controlled production of micromaterials, thereby aiding its widespread adoption.

Supplementary Material

Refer to Web version on PubMed Central for supplementary material.

Acknowledgements

The authors acknowledge prof. P.J. Dijkstra for his help with Dex-TA synthesis. MK acknowledges financial support from the Dutch Arthritis Foundation (#LLP-25). JL acknowledges financial support from an Innovative Research Incentives Scheme Veni award (#14328) from the Netherlands Organization for Scientific Research (NWO), the European Research Council (ERC, Starting Grant, #759425), and the Dutch Arthritis Foundation (#17–1-405). Conception by TK, SH, and JL. Experimental design by TK, BvL, and JL. Experiments performed by TK, BvL, and MG. Data interpretation by all authors. Manuscript written by TK and JL. Supervision and revisions by TK, MK, and JL.

References

1. Whitesides GM, The origins and the future of microfluidics. Nature, 2006 442(7101): p. 368–73. [PubMed: 16871203]
2. Ma S, et al., Fabrication of microgel particles with complex shape via selective polymerization of aqueous two-phase systems. Small, 2012 8(15): p. 2356–60. [PubMed: 22648761]

3. Kang E, et al., Digitally tunable physicochemical coding of material composition and topography in continuous microfibres. Nat Mater, 2011 10(11): p. 877–83. [PubMed: 21892177]
4. Xu S, et al., Generation of monodisperse particles by using microfluidics: control over size, shape, and composition. Angew Chem Int Ed Engl, 2005 44(5): p. 724–8. [PubMed: 15612064]
5. Temiz Y, et al., Lab-on-a-chip devices: How to close and plug the lab? Microelectronic Engineering, 2015 132: p. 156–175.
6. Fiorini GS and Chiu DT, Disposable microfluidic devices: fabrication, function, and application. BioTechniques, 2005 38(3): p. 429–446. [PubMed: 15786809]
7. Bauer WA, et al., Hydrophilic PDMS microchannels for high-throughput formation of oil-in-water microdroplets and water-in-oil-in-water double emulsions. Lab Chip, 2010 10(14): p. 1814–9. [PubMed: 20442967]
8. Anna SL, Droplets and Bubbles in Microfluidic Devices. Annual Review of Fluid Mechanics, 2016 48(1): p. 285–309.
9. Holtze C, Large-scale droplet production in microfluidic devices-an industrial perspective. Journal of Physics D-Applied Physics, 2013 46(11).
10. Holtze C, Weisse AS, and Vranceanu M, Commercial Value and Challenges of Drop-Based Microfluidic Screening Platforms–An Opinion. Micromachines, 2017 8(6).
11. Terray A and Hart SJ, “Off-the-shelf” 3-D microfluidic nozzle. Lab on a Chip, 2010 10(13): p. 1729–1731. [PubMed: 20376381]
12. Li T, et al., Simple and reusable off-the-shelf microfluidic devices for the versatile generation of droplets. Lab on a Chip, 2016 16(24): p. 4718–4724. [PubMed: 27809329]
13. Wang Y, et al., Controllable geometry-mediated droplet fission using “off-the-shelf” capillary microfluidics device. RSC Advances, 2014 4(59): p. 31184–31187.
14. Bottaro E and Nastruzzi C, “Off-the-shelf” microfluidic devices for the production of liposomes for drug delivery. Materials Science and Engineering: C, 2016 64: p. 29–33. [PubMed: 27127025]
15. Wang K, et al., Generation of micromonodispersed droplets and bubbles in the capillary embedded T-junction microfluidic devices. AIChE Journal, 2011 57(2): p. 299–306.
16. Kamperman T, et al., Single Cell Microgel Based Modular Bioinks for Uncoupled Cellular Micro- and Macroenvironments. Adv Healthc Mater, 2017 6(3).
17. Dekker S, et al., Standardized and modular microfluidic platform for fast Lab on Chip system development. Sensors and Actuators B: Chemical, 2018 272: p. 468–478.
18. Kevin V and Abraham Phillip L, A truly Lego ® -like modular microfluidics platform. Journal of Micromechanics and Microengineering, 2017 27(3): p. 035004.
19. Owens CE and Hart AJ, High-precision modular microfluidics by micromilling of interlocking injection-molded blocks. Lab on a Chip, 2018 18(6): p. 890–901. [PubMed: 29372201]
20. Bhargava KC, Thompson B, and Malmstadt N, Discrete elements for 3D microfluidics. Proc Natl Acad Sci U S A, 2014 111(42): p. 15013–8. [PubMed: 25246553]
21. Guckenberger DJ, et al., Micromilling: a method for ultra-rapid prototyping of plastic microfluidic devices. Lab Chip, 2015 15(11): p. 2364–78. [PubMed: 25906246]
22. Kamperman T, et al., Centering Single Cells in Microgels via Delayed Crosslinking Supports Long-Term 3D Culture by Preventing Cell Escape. Small, 2017 13(22): p. 1603711-n/a.
23. Park JI, et al., Microfluidic Synthesis of Polymer and Inorganic Particulate Materials. Annual Review of Materials Research, 2010 40(1): p. 415–443.
24. Christopher GF, et al., Experimental observations of the squeezing-to-dripping transition in T-shaped microfluidic junctions. Physical Review E, 2008 78(3): p. 036317.
25. Nunes JK, et al., Dripping and jetting in microfluidic multiphase flows applied to particle and fiber synthesis. J Phys D Appl Phys, 2013 46(11).
26. Zagnoni M, Anderson J, and Cooper JM, Hysteresis in multiphase microfluidics at a T-junction. Langmuir, 2010 26(12): p. 9416–22. [PubMed: 20465264]
27. Yobas L, et al., High-performance flow-focusing geometry for spontaneous generation of monodispersed droplets. Lab on a Chip, 2006 6(8): p. 1073–1079. [PubMed: 16874381]
28. Anna SL, Bontoux N, and Stone HA, Formation of dispersions using “flow focusing” in microchannels. Applied Physics Letters, 2003 82(3): p. 364–366.

29. Wacker J, Parashar VK, and Gijs MAM, Influence of Oil Type and Viscosity on Droplet Size in a Flow Focusing Microfluidic Device. Procedia Chemistry, 2009 1(1): p. 1083–1086.
30. Papirer E, Adsorption on silica surfaces. 2000: Marcel Dekker, Inc.
31. Ogden MW and McNair HM, Characterization of fused-silica capillary tubing by contact angle measurements. Journal of Chromatography A, 1986 354: p. 7–18.
32. Seiffert S, et al., Reduced UV light scattering in PDMS microfluidic devices. Lab Chip, 2011 11(5): p. 966–8. [PubMed: 21218249]
33. Wang S, et al., An in-situ photocrosslinking microfluidic technique to generate non-spherical, cytocompatible, degradable, monodisperse alginate microgels for chondrocyte encapsulation. Biomicrofluidics, 2018 12(1): p. 014106. [PubMed: 29375727]
34. Wang S, et al., A Very Low-Cost, Labor-Efficient, and Simple Method to Block Scattered Ultraviolet Light in PDMS Microfluidic Devices by Inserting Aluminum Foil Strips. Journal of Thermal Science and Engineering Applications, 2018 11(1): p. 014501–014501-3.
35. Kamperman T, et al., Nanoemulsion-induced enzymatic crosslinking of tyramine-functionalized polymer droplets. Journal of Materials Chemistry B, 2017 5(25): p. 4835–4844.
36. Ashida T, Sakai S, and Taya M, Competing two enzymatic reactions realizing one-step preparation of cell-enclosing duplex microcapsules. Biotechnol Prog, 2013 29(6): p. 1528–34. [PubMed: 23955874]
37. Tan WH and Takeuchi S, Monodisperse Alginate Hydrogel Microbeads for Cell Encapsulation. Advanced Materials, 2007 19(18): p. 2696–2701.

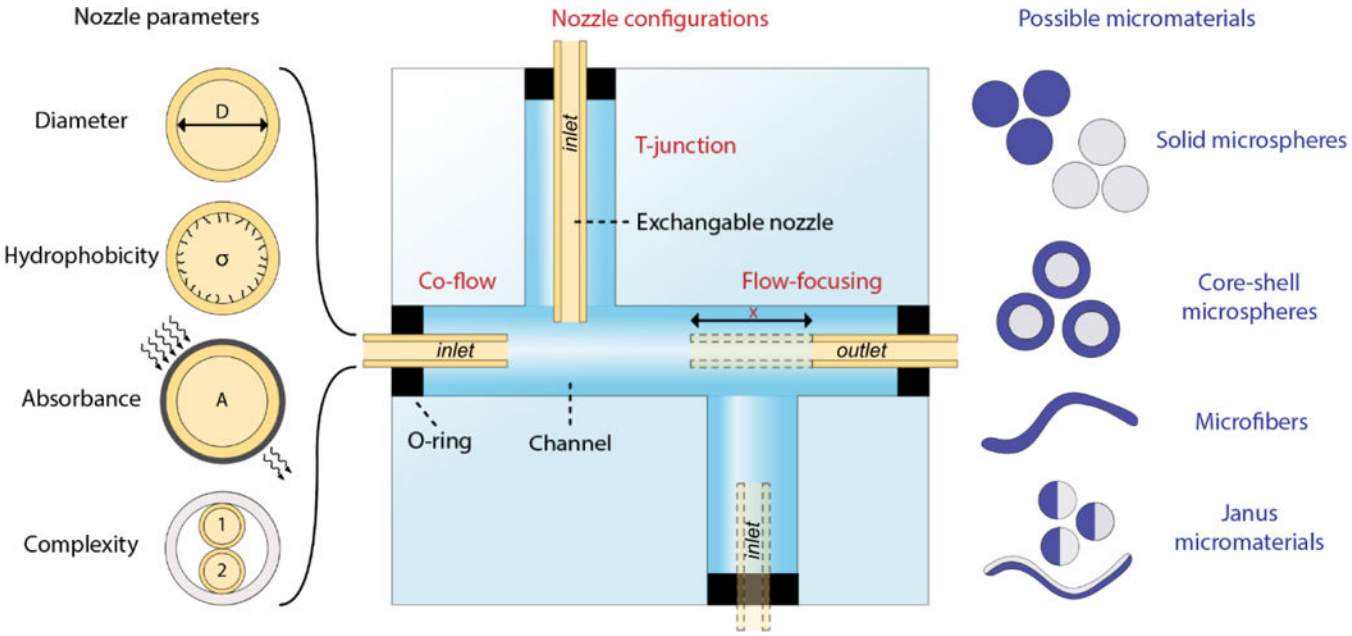

Figure 1. Schematic concept of exchangeable nozzles within a multifunctional 3D microfluidic device for versatile monodisperse micromaterials production.

Sealed connections between the device, tubing, and nozzles enable the on-the-fly exchangeable of nozzles. This allows for the on-demand switching between nozzles with different diameters, hydrophobicity, absorbance, and complexity. Furthermore, the nozzle placement can be temporally controlled to switch between T-junction, co-flow, and flow-focusing configurations. The multifunctional nature of this microfluidic device enables facile tuning towards the fabrication of various micromaterials including emulsions, microspheres, and microfibers.

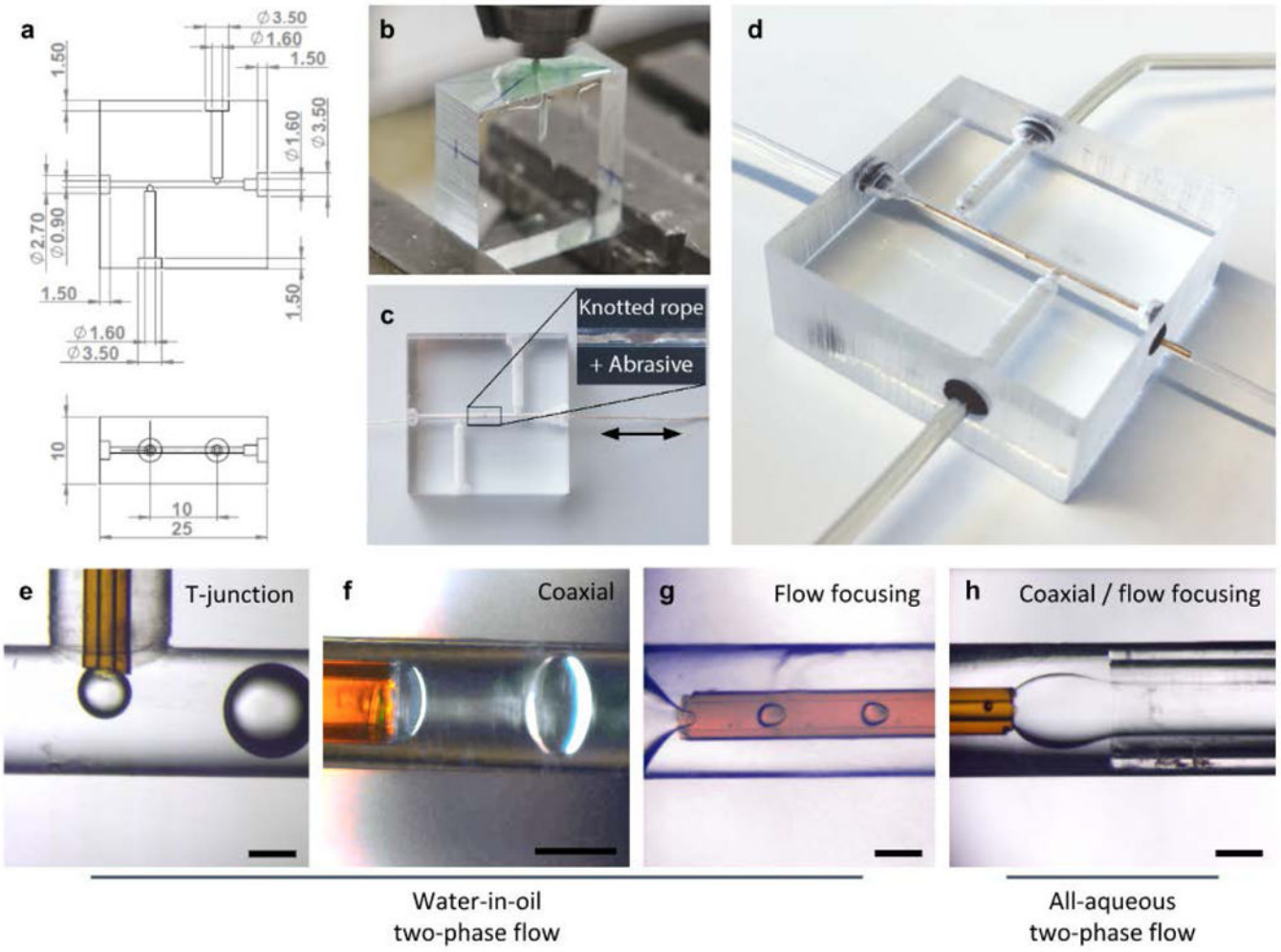

Figure 2. Engineering a microfluidic device with exchangeable nozzles.

(**a**) Computer-aided design (CAD) of the multifunctional 3D microfluidic device. The device was fabricated in PMMA using standard (**b**) cutting (i.e., sawing and micromilling) and (**c**) abrasion (i.e., polishing) techniques. (**d**) Tubing and nozzles were sealed to the PMMA device using rubber O-rings that auto-centered inserted nozzles. The adaptable nature of the microfluidic device enabled the straightforward generation of water-in-oil and all-aqueous two-phase flows using (**e**) T-junction, (**f**) coaxial, (**g**) flow focusing, and (**h**) coaxial / flow focusing nozzle configurations. Scale bars indicate 350 μm.

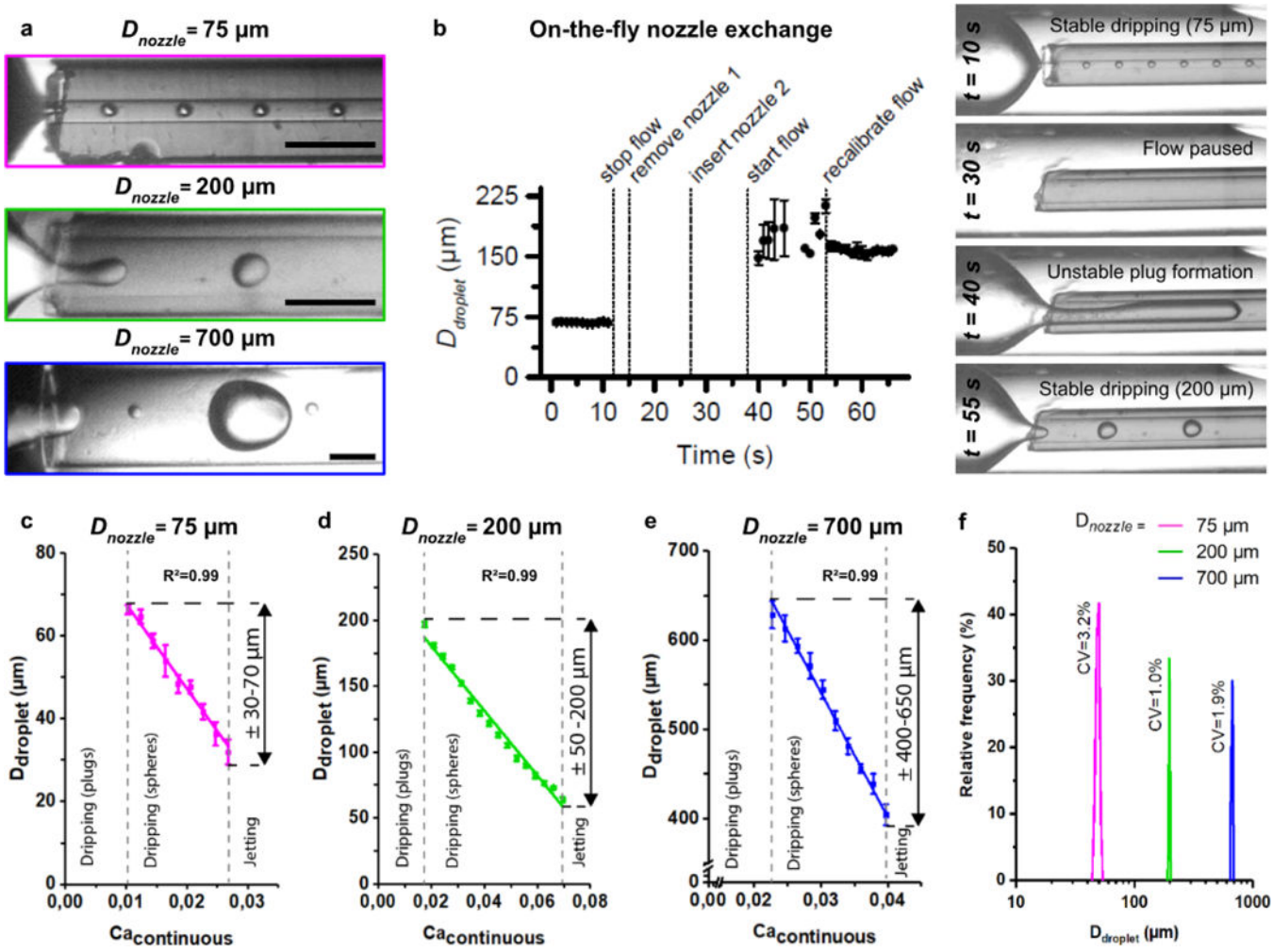

Figure 3. Characterization of microdroplets production with on-the-fly nozzle exchange.

(**a**) Coaxially flowing water in oil using nozzles with different inner diameters enabled the formation of droplets with diameters spanning more than an order of magnitude. (**b**) Switching between two stable droplet production size regimes by exchanging the nozzle was achieved within one minute. (**c-e**) Per nozzle, the droplet size was fine-tuned by tuning the flow rate and thereby the capillary number of the continuous phase. (**f**) All nozzles were compatible with the production of monodisperse (CV <5%) droplets. Scale bars indicate 350 µm.

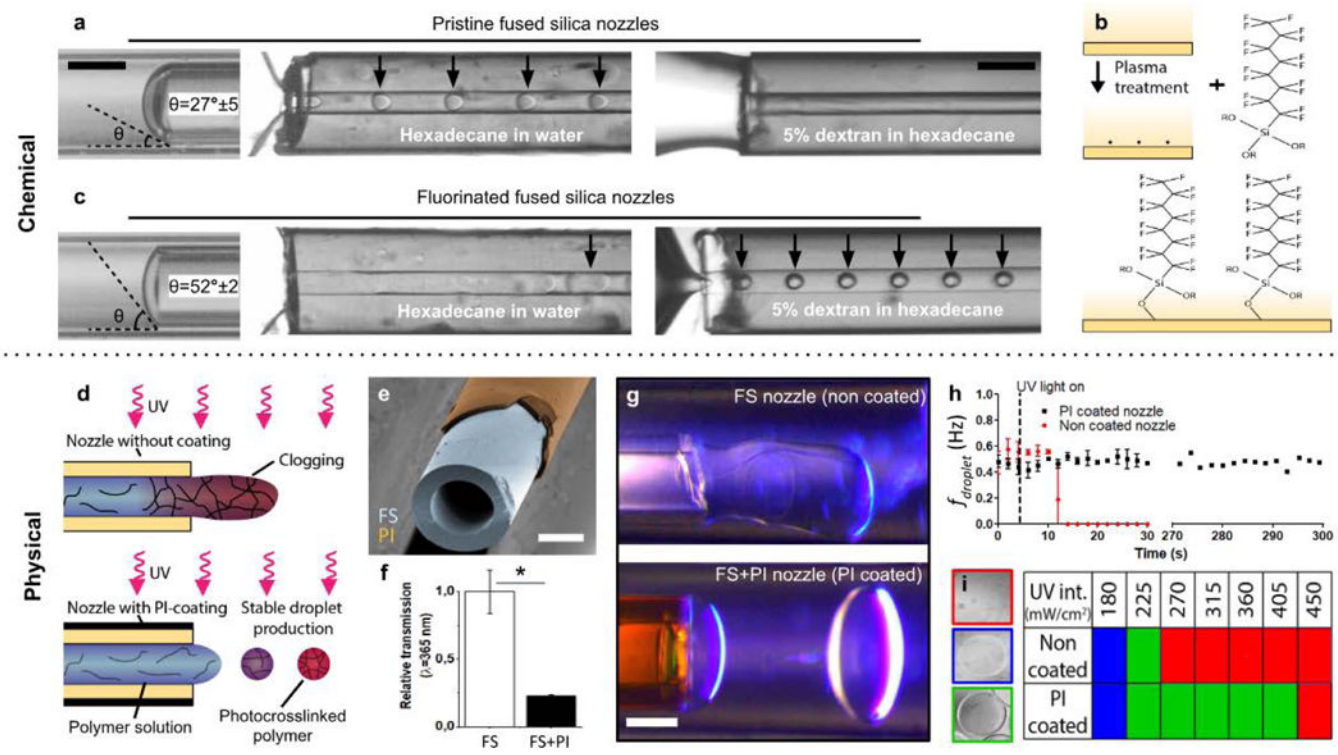

Figure 4. Chemical and physical optimization of exchangeable nozzles to enable the processing of polymers solutions.

(**a**) Pristine fused silica nozzles were hydrophilic, which readily enabled the formation of O/W emulsions, but impaired the formation of polymer-laden W/O emulsions such as dextran solution in hexadecane. (**b**) Chemically treating the fused silica with fluorinated silane (**c**) resulted in less hydrophilic nozzles that were compatible with the production of polymer-laden W/O emulsions. (**d-e**) Alternatively, fused silica (FS) nozzles could be physically modified with a UV-protective polyimide (PI) coating to prevent nozzle clogging during processing of photocrosslinkable polymers. (**f**) The polyimide coating reduced the relative UV transmission by more than 4-fold and enabled (**g,h**) continuous and stable production of photocrosslinked polymer microspheres under UV irradiation by preventing nozzle clogging (**i**) over a wide range of UV intensities as compared to non-coated nozzles. Nozzle clogging, incompletely photocrosslinked PEGDA, and completely photocrosslinked PEGDA are indicated with red, blue, and green squares, respectively. Scale bars indicate 200 μm. * indicates significance with $p < 0.01$.

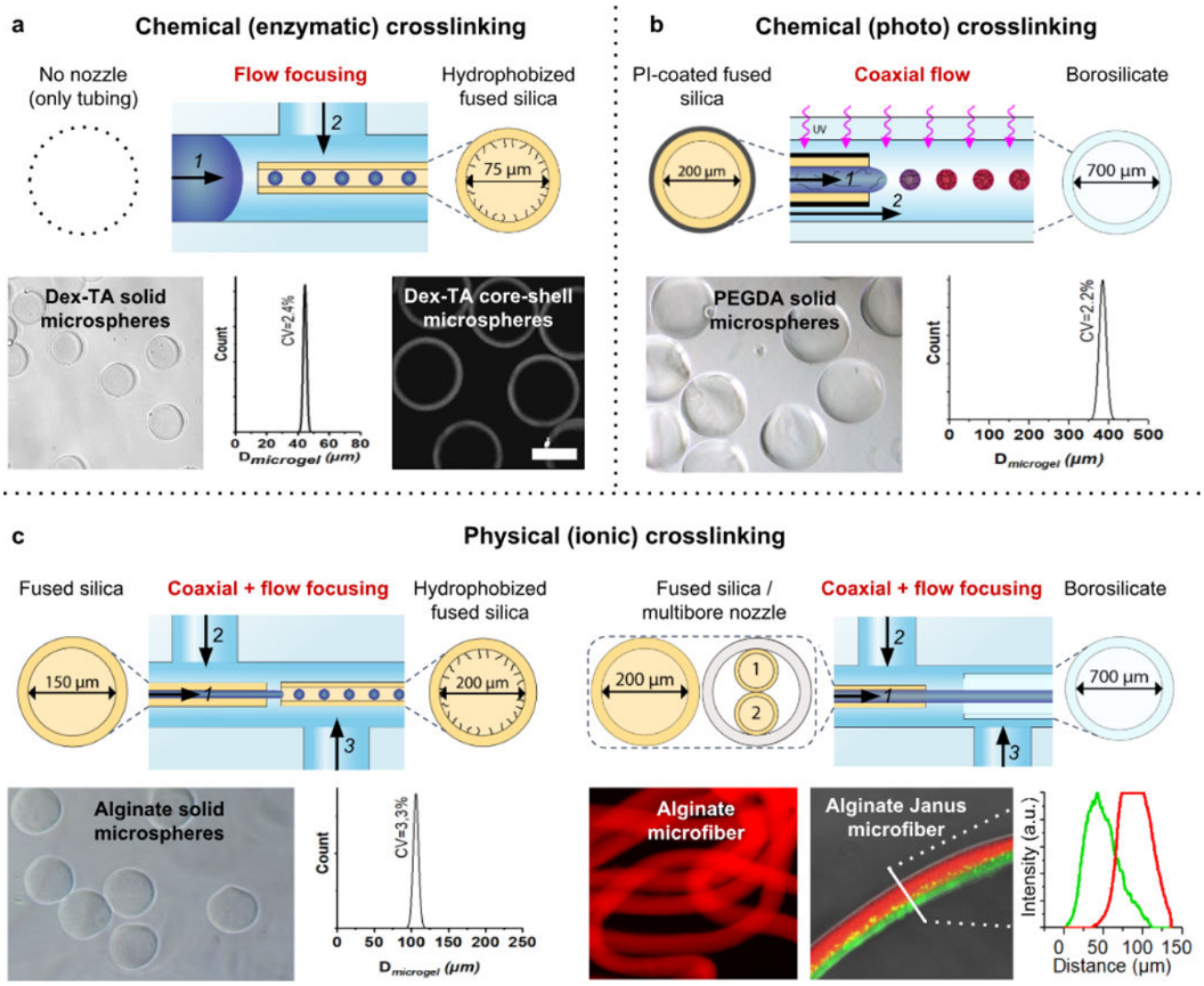

Figure 5. Various examples of monodisperse micromaterials produced using the multifunctional 3D microfluidic device with different optimized nozzle configurations.

(**a**) Flow focusing an enzymatically crosslinkable Dex-TA and HRP containing solution (*1*) in hexadecane with Span 80 (*2*) using a fluorinated fused silica nozzle enabled the production of monodisperse solid dextran-based microspheres. (**b**) Coaxially flowing a photocrosslinkable PEGDA and I2959 containing solution (*1*) in hexadecane with Span 80 (*2*) using a polyimide-coated fused silica nozzle enabled the production of monodisperse PEG-based microspheres. (**c**) Focusing coaxially flowing alginate (*1*) and PEG (*2*) containing solutions in a calcium chloride containing solution (*3*) using a combination of single and multibore capillaries enabled the production of monodisperse simple and Janus type microfibers. Scale bar indicates 200 µm.